Information in Phase of Beta Band of Motor Cortex Generated Actions

Physics 256A&B, Spring 2013

Preeya Khanna
UCB-UCSF JGG in Bioengineering
pkhanna@berkeley.edu

ABSTRACT

Strong oscillations present in local field potential (LFP) recordings at specific frequencies are thought to be involved in behavior, communication, and coordination across brain areas. In this dataset, the use of inter-regional phase differences to control a brain-machine interface (BMI) is studied. The task is a one-dimensional two-target task where phase differences extracted from distal electrodes in left motor cortex (M1) and right dorsal pre-motor cortex (PMd) at a frequency of 30 Hz is mapped to velocity of a cursor. The subject is able to volitionally control the cursor, and we model the strategy he uses with a coupled oscillator model. By comparing the model to the measure phase data using information theoretic values, we concluded that that the volitional control of phase is not well accounted for by coupling strength of oscillators and Gaussian noise alone.

I. Introduction

Low frequency oscillations *in vivo* have been measured with invasive methods such as cortical electrode local field potentials (LFPs), less invasive methods such as electrocorticography (ECog), as well as non-invasive methods such as electroencephalography (EEG). Oscillations are present in all measurement modalities and are prominent in specific frequency bands during stereotyped behaviors. One often-reported oscillation in motor cortex is termed the 'beta band' (20-40 Hz) and occurs during initiation of movement, dexterous movement, and motor cortex controlled brain-machine interfaces (Fetz, 2013). Theories postulating the role, of oscillations in neural computations are widespread, but few have investigated experimentally the robustness of these recorded oscillations. While they are certainly well reported, how sensitive they are perturbation and how strongly coupled they are across distal regions of the brain has not been explored. In this project, I explore a dataset where we implement an operant-conditioned paradigm in the form of a brain-machine interface to determine if phase coupling can be volitionally controlled. Phase across hemispheres was shown to volitionally controllable.

In this report, the phase difference used to drive the BMI in the experiment was modeled using a coupled oscillator dynamical system. System parameters were fit to minimize discrepancy in information theoretic values between the measured and simulated data. Epsilon machines were then calculated using the sub-tree algorithm to analyze and compare the causal states of both processes. The conclusion was that the coupled oscillator model while matching the basic information theoretic values of the phase BMI process did not account for the low entropy rate and high excess entropy, and another model was suggested for analysis.

II. Background

Mechanisms of neural computation are heavily debated. While the neuron and its action potential are accepted as the units of computation in the brain, the manner in which neurons work together to encode and transmit information through their action potentials is unclear. However, an emerging hypothesis is that low frequency oscillations in the brain may represent summed neural assemblies working together synchronously. Neurons firing synchronously have been postulated to have been postulated to enable communication across distal brain regions, may be involved in hierarchal processing, and may also be a physical manifestation of internally-directed attention in the brain.

Some the most powerful evidence for the low frequency oscillations containing relevant neuron information comes from *in vitro* cortical slice preparation. In particular, it has been found that when slow (0.5-1.5 Hz) oscillatory electric fields are applied with parallel plates across a cortical slice neurons in the slice tend to modulate their spikes such that their interspike interval matches the period of the global oscillation. If these oscillations were irrelevant to neural spiking, it is highly improbably that organization around the oscillations would occur. Other studies using pharmacological agents have shown that in slice, very specific frequencies can be generated ranging from slow delta waves (~1Hz) to faster gamma waves (~60Hz) (Roopun et al., 2008). The frequencies

generated are not arbitrary, but rather tend to match the same measured frequencies bands strongly present in *in vivo* systems. One effect from neurons reorganizing their firing rate with respect to the ongoing global oscillation is that spikes exhibit a preferred phase. This effect has been shown *in vivo* as well, where place cells in hippocampus fire at a specific phase of the ongoing theta (8-12 Hz) oscillation (Buzsaki and Draguhn).

The relative phase of ongoing oscillations has been shown to be relevant not just in hippocampus place cells, but across motor cortex as well. In motor cortex, spatial travelling waves of beta oscillations have been shown to propagate in primary motor cortex (M1) and dorsal pre-motor cortex (PMd) during motor preparation (Rubino et al., 2006). However, what remains unclear is how tightly coupled oscillations that arise in different areas are to each other, and what role if any such phase-locking plays in neural computation.

To study phase locking of oscillations *in vivo*, a closed-loop brain-machine interface (BMI) task was used. In this setup, subjects receive feedback of their neural activity mapped into a task, and are rewarded for specific neural modulation patterns. Canonically, BMI has relied on modulation of the firing rate of single neurons. However, volitional modulation of low-gamma LFP power has recently been demonstrated. This result inspired the use phase of LFPs as a BMI control signal to: 1) determine if it is possible to modulate the phase relationship of ongoing LFPs, and 2) to probe the degree of flexibility of these relationships across motor cortex. In this 'Phase-BMI' task, phase differences between two distal regions of motor cortex control the velocity of a cursor confined to moving on a one -dimensional line toward targets for a liquid reward. Below is a figure illustrating the task setup.

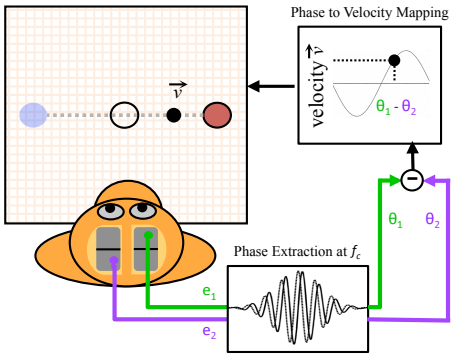

Subject has recordings from L M1, R PMd and the phase of these is calculated using a chirplet transform. Phase difference between the electrodes is mapped to cursor velocity. The subject attempts to modulate the cursor either left or right.

The subject was able to acquire a significantly higher number of targets than he would by chance. Data from a session of peak performance is analyzed.

III. Dynamical System:

I. Overview: In this project I used data from the best session (most targets obtained in 10 min) of a subject performing Phase-BMI at 30 Hz. I first investigated my data by calculating the entropy and mutual information of the phase distributions that I emerged with. I then investigated coupled oscillator models and selected parameters to fit

my data to a coupled oscillator model. I then interpreted my fit model and real data by evaluating their underlying epsilon machines, statistical complexity, and entropy rates.

II. Description -- Coupled Oscillators: Coupled oscillator models have been used to describe phase interactions of neural oscillations by many (Cadieu and Koepsell, 2010; Canolty et al., 2010). In its simplest form two coupled oscillators can be described by the following dynamical system:

$$\frac{\partial \theta_1}{\partial t}(t) = \omega - \kappa_{12}\sin(\theta_1 - \theta_2 - \mu_{12}) + \nu_1(t)$$

$$\frac{\partial \theta_2}{\partial t}(t) = \omega - \kappa_{21}\sin(\theta_2 - \theta_1 - \mu_{21}) + \nu_2(t)$$

Here ω is the center frequency of the oscillator, κ_{ij} is the coupling strength between oscillator *i* and oscillator *j* (this term has directionality – κ_{ij} is the effect of oscillator *j* on oscillator *i*), μ_{ij} is the natural phase offset between oscillator *i* and oscillator *j* and $\nu_i(t)$ is the noise term.

This dynamical system is a natural one to consider when since trying to understand phase differences between oscillations. If a coupled oscillator can be fit well to data, understanding of phase interactions between different parts of the brain can be interpreted as changes in coupling strength, natural offset, and noise coefficients. One way to interpret this Phase –BMI task in terms of the coupled oscillator is model is to attribute the synchrony of two channels to the coupling strength κ, interpret μ as a value that shifts depending on which target is present (see below), and ν as an aggregated value accounting for the stochastic nature of neural activity and possible electrical noise in neural recordings.

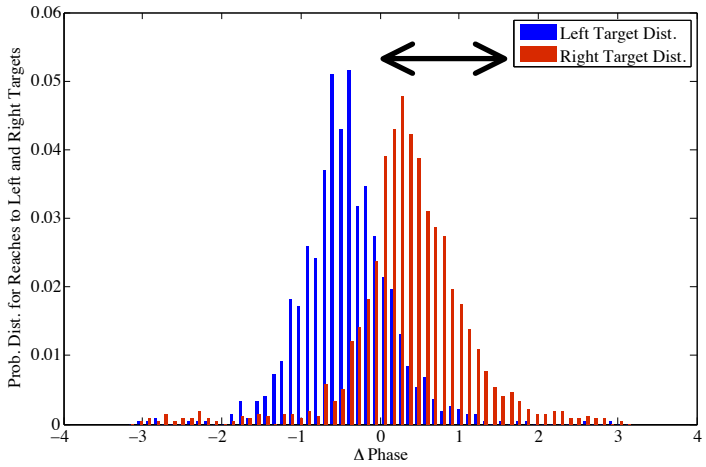

Histogram showing the distribution of phase differences during reaches to the right target and reaches to left target. A coupled oscillator model could reflect this shift by taking different values of μ for each reaching condition.

IV: Methods

Fitting the coupled oscillator model optimally was not an avenue that was heavily investigated. Closed-form maximum entropy derivations are fleshed out in literature (Cadieu and Koepsell, 2010). Instead, the model was simplified by setting $\omega_1 = \omega_2$, and $\mu_{12} = \mu_{21} = 0$. Fit of the model was then evaluated by comparing it to real data, using entropy and KL divergence as a metric of similarity. Since the goal was to better understand underlying states in phase differences during BMI, as long as the model produced a distribution that resembled the one from data, the outcome would be informative.

After fitting the model, the underlying states of both processes were investigated. To do this, data was partitioned using a task-relevant division. Phase differences greater than zero move the cursor to the right (and were coded as a '1') and phase differences less than zero move the cursor left (and were coded as a '0'). Underlying causal states were then calculated using the subtree algorithm.

V: Results

I. Information Theory Values: There are two channels; electrode 1 and electrode 2. To control the BMI task in realtime phase for both channels was calculated, and their difference was recorded.

Entropy – When considering individual channels, since phase is a circular variable with respect to an ongoing oscillation, I expect that the entropy of the phase distribution for a single channel will be largely uniform. For channels 1 and 2 shown below, the entropy of both distributions is **5.9069** bits, which is equal to maximum entropy of - $\log_2(1/n)$.

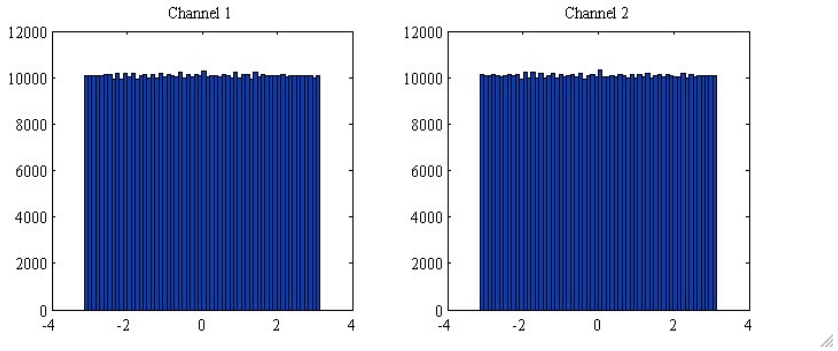

On the other hand, when the difference between the phases is considered (below right), there is certainly more information. The entropy of the phase differences is **5.4454** bits. Clearly, there is more information in considering the difference between phases than in just considering phases themselves.

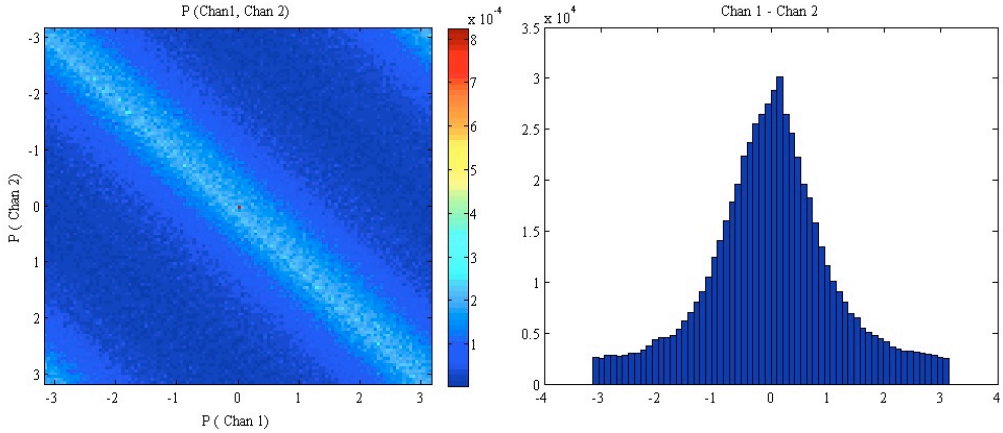

Mutual Information –It appears that there is information contained in the differences between the phases of the two channels, and we can quantify that by calculating the mutual information between them. The mutual information between the two distributions is **0.7055 bits**. For visualization, the joint distribution, of both channels is shown above (left). Clearly the channels are frequently in synchrony illustrated by the lighter diagonal line indicating a higher probability that both channels are the same value. Also note worth are the top right and bottom left edges, indicating that when the channels are not synchronized, they are likely to be fully un-synchronized. The low amount of mutual information means that there is still quite a bit of randomness in each channel, such that H (channel 1 | channel 2) = H (channel 1) – I (channel 1 ; channel 2) = 5.9069 bits - 0.7055 bits = **5.2014 bits**. Thus the entropy of the phase of one channel given that we know the phase of the other channel (5.2014 bits) is lower than the entropy of the difference between the two channels (5.4454 bits). This is interesting because knowing the phase of one channel gives more information about the phase of the other channel, than just knowing that the two channels in general happen to be synchronized frequently.

II. Fitting the Dynamical System

Below are some brief results from fitting the dynamical system to the data:

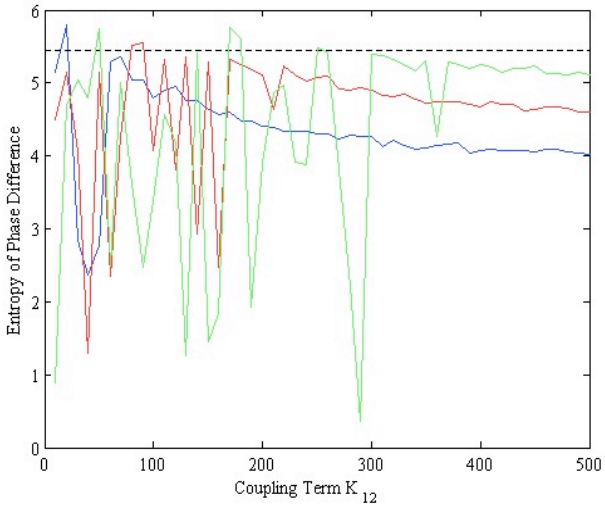

Fitting Fig 1: Effect of different coupling terms and noise terms (blue: ν =1000, red: ν =1500, green: ν =2000) on the entropy of the phase difference distribution. Entropy of real data is shown as a black dotted line.

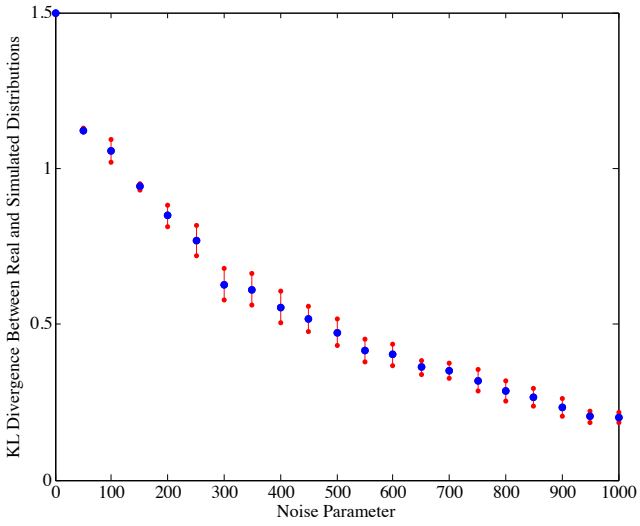

Fitting Fig 2: KL divergence between real and simulated data as a function of increasing noise. Each condition was simulated 100 times (red bars are standard deviation). A noisier coupled oscillator produces distributions more similar to actual data.

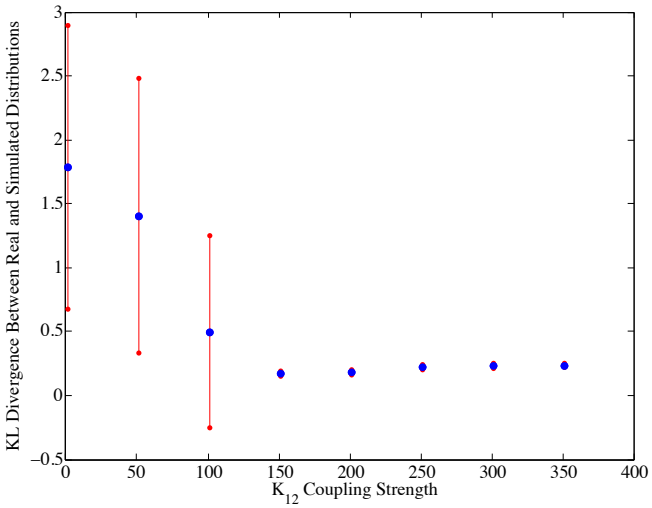

Fitting Fig 3: KL divergence between real and simulated data as a function of increasing coupling. Each condition was simulated 100 times (red bars are standard deviation). There appears to be a minimum representing the lowest KL divergence around a coupling strength of 150

Generally as coupling increases, the entropy of the distribution drops, which is expected since as coupling occurs, the difference in phases will become less random and more

consistently zero. I approximated the best parameters that matched the data as κ = 100, ν = 1000, and μ = 0 (for baseline data – not reaching to targets in either direction). The output of the coupled oscillator with these values is shown below:

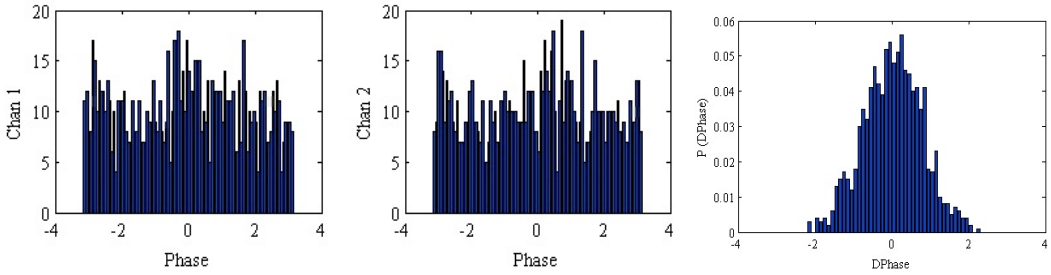

Absolute phase of Channels 1 and 2 (left, center), and difference of phases (right). Below is real data and simulated data (same as above, right) plotted together.

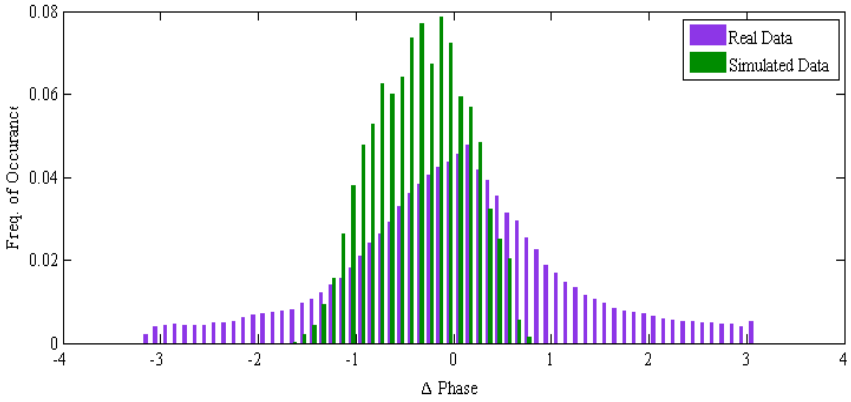

Finally, a comparison below of the time-series trajectories of difference of phase for real (left) and simulated (right) data. One obvious difference is the way in which real data smoothly varies, and simulated data appears more 'jittery'. Since much of the variation in the simulated model is from the Gaussian noise term, there is not consistency from time point to time point. On the other hand, the real data (left) appears to have much stronger structure where variation is not due to noise since each point is well correlated with points near it.

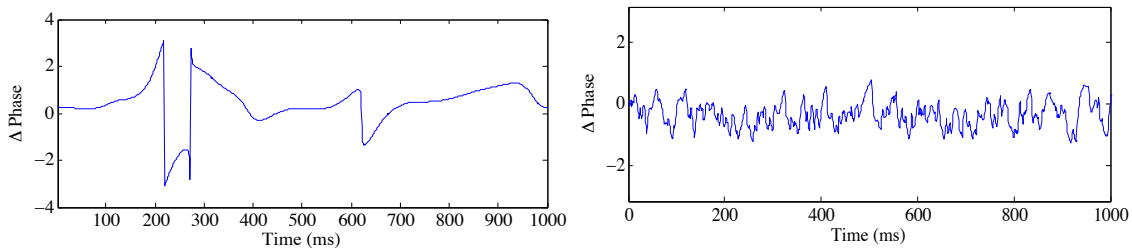

III. Causal States

The subtree method with a morph length of 3 and tree depth of 5 was used to estimate the epsilon machine. These short lengths were initially chosen to quantitatively investigate the obvious differences between real and simulated data in their smoothness.

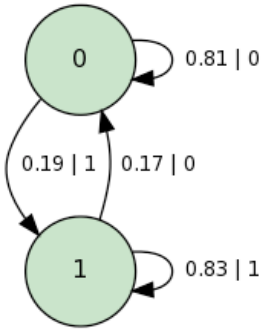

Simulated Data;

	hμ	Cμ	E
Inferred Machine	0.67342	0.99843	0.32501

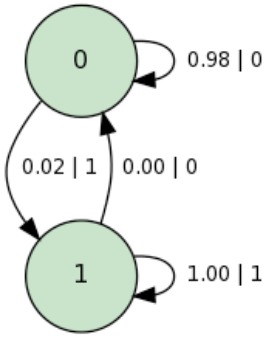

Real Data;

	hμ	Cμ	E
Inferred Machine	0.05040	0.65118	0.60078

The above machines illustrate the qualitative observation concerning the difference between the real and simulated data. The huge differences are reflected in the differences between entropy rates. For the simulated data, the process is much more random for each time point compared to the real data. The excess entropy of the machines is also reflective of the different sources of randomness in the two different processes. While excess entropy mostly contributes to statistical complexity in the real data, entropy rate is mostly responsible for statistical complexity in the simulated data. Interestingly, the entropy rate of the simulated data is on the same order of magnitude as the excess entropy in the real data. This may be suggesting that the observed measures of entropy and KL divergence that I attempted to optimize while adjusting parameters of the coupled oscillator model may have actually been a result of excess entropy in the real system.

VI: Conclusion

The conclusion of these simulations is that in order to model the phase difference from the Phase –BMI task described, Gaussian noise with coupling is not sufficient. Other mechanisms must be underlying the process in order to account for the high entropy yet highly structured, smooth signal. One possibility is that the animal is exerting discrete pulses to move the cursor with his neural activity. These ‘pulses’ exude a stereotyped impulse response from the system, which allows him to control the cursor. The idea of impulse responses in neurons has been explored through literature describing “phase resetting” of oscillators due to external stimuli. Neurons that fire periodically will

reset their phase in a well-defined manner in response to external stimuli. To describe the neuron's resetting behavior, phase resetting curves can be calculated that illustrate how the neuron changes its next firing depending on when in the cycle the external stimuli fires. For example, below is a phase resetting curve for a cortical neuron.

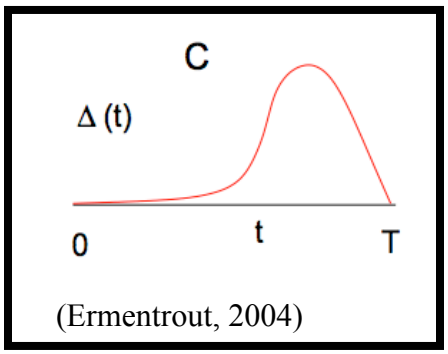

(Ermentrout, 2004)

Phase Resetting Curve: The change in the firing pattern (y axis) of the neuron that is firing with a period of T is related to when in the neuron's period (between 0sec and T sec) the external stimuli. For this neuron, stimuli that occur later in the cycle cause the neuron to "wait" to fire after it normally would. Stimuli occurring early in the period have little effect.

This paradigm could be applied to phase-BMI models as well. Potentially, as the subject attempts to reach to the right or left, he could perturb the synchronized phase of the two oscillators and the phase would respond in a smooth, stereotyped way. This type of response may be a more accurate way to maintain the high entropy that phase-BMI data exhibits, but also maintain a low entropy rate in the way that Gaussian noise was unable to.

VII: Sources Cited:

Buzsaki, G., and Draguhn, A. Neuronal Oscillations in Cortical Networks.

Cadieu, C.F., and Koepsell, K. (2010). Phase coupling estimation from multivariate phase statistics. Neural Comput *22*, 3107–3126.

Canolty, R.T., Ganguly, K., Kennerley, S.W., Cadieu, C.F., Koepsell, K., Wallis, J.D., and Carmena, J.M. (2010). Oscillatory phase coupling coordinates anatomically dispersed functional cell assemblies. Proc. Natl. Acad. Sci.

Fetz, E.E. (2013). Volitional Control of Cortical Oscillations and Synchrony. Neuron *77*, 216–218.

Roopun, A.K., Kramer, M.A., Carracedo, L.M., Kaiser, M., Davies, C.H., Traub, R.D., Kopell, N.J., and Whittington, M.A. (2008). Temporal Interactions between Cortical Rhythms. Front. Neurosci. *2*, 145–154.

Rubino, D., Robbins, K.A., and Hatsopoulos, N.G. (2006). Propagating waves mediate information transfer in the motor cortex. Nat. Neurosci. *9*, 1549–1557.